

## Boron carbide–copper infiltrated cermets

S. Tariolle,<sup>a</sup> F. Thévenot,<sup>a</sup> M. Aizenstein,<sup>b</sup> M.P. Dariel,<sup>b,\*</sup> N. Frumin,<sup>b</sup> and N. Frage<sup>b</sup>

<sup>a</sup> *Laboratoire Céramiques Spéciales, ENS des Mines de Saint-Etienne, France*

<sup>b</sup> *Department of Materials Engineering, Faculty of Engineering Science, Ben-Gurion University of the Negev, P.O. Box 653, 84105 Beer-Sheeva, Israel*

Received 1 October 2002; accepted 13 February 2003

### Abstract

Porous boron carbide preforms, prepared with and without excess carbon, were infiltrated with a Cu–Si alloy. Contrary to unalloyed copper, the Cu–Si alloy wets and infiltrates the porous preforms. A thermodynamic analysis of the B–C–Cu–Si system indicated that a Si content of the alloy above 15 at% leads to the formation of SiC. At higher Si content, the composition of boron carbide in contact with the melt also changes towards higher boron content. Metallographic examination validated these conclusions. The SiC compound forms preferentially around the free carbon particles in preforms containing excess carbon, and also in the vicinity of carbide that did not contain any excess carbon. Eventually, SiC, a product of the reaction between the carbide and the melt, forms a continuous barrier that impedes completion of the reaction and accounts for the limited increase of hardness as a result of lengthy heat treatments.

© 2003 Elsevier Inc. All rights reserved.

**Keywords:** Boron carbide; B<sub>4</sub>C–Cu cermets; Infiltrated cermets; SiC

### 1. Introduction

Boron carbide-based ceramic–metal composites may, in principle, provide a useful combination of the elevated hardness of the ceramic with some toughness due to the metal component. One approach for the fabrication of such composites is based on the infiltration of the ceramic preform having a controlled fraction of porosity with a molten metal or alloy. Thus boron carbide–aluminum composites have attracted considerable interest, in particular, due to their low specific weight [1–3]. One drawback of these composites is the appearance of the undesirable Al<sub>4</sub>C<sub>3</sub> phase that, on account of its instability in ambient atmosphere, may cause the decomposition of the material. Boron carbide infiltrated with Cu is another potentially useful composite that has somewhat higher specific weight but may present useful electrical and thermal conductivity properties. Preliminary experiments have revealed significant problems involved with the infiltration of B<sub>4</sub>C by molten Cu owing to the apparent lack of wetting in this system. Many efforts have been made in order to

circumvent this difficulty. Thus Pyzik and Nilsson [4] suggested pressure-assisted infiltration, and Maruyama and Onose [5] used copper-coated B<sub>4</sub>C particles, as starting materials. Since these solutions are not particularly cost-effective, it was decided to adopt a different approach, based on a close examination of the microstructure of the B<sub>4</sub>C–copper interface. In particular, it appeared that molten Cu attacks B<sub>4</sub>C by having boron dissolve in the molten metal, forming a crater and leaving behind a carbon residue [6]. This latter forms a layer that prevents further wetting of the ceramic and impedes the completion of the Cu infiltration process. Thus, the crater formation was attributed to the dissociation of the boron carbide accompanied by carbon precipitation as graphite. The carbon released from the carbide floats upward into the melt and forms agglomerates. Boron that is released dissolves in the liquid metal and in the course of solidification, precipitates in the copper matrix.

The different approach that was adopted was based on the premise that by suitable alloying of the molten metal, the infiltration-inhibiting lack of wetting could be resolved and a suitable microstructure of the interface generated. A not less important consideration was the expected contribution of the alloying elements to the

\*Corresponding author. Fax: 972-8-647-714.

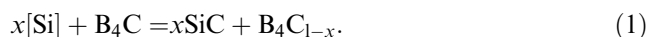
E-mail address: [dariel@bgumail.bgu.ac.il](mailto:dariel@bgumail.bgu.ac.il) (M.P. Dariel).

post-infiltration performance of the resulting composite. Silicon appeared to be a suitable candidate fulfilling these requirements. A preliminary thermodynamic analysis confirmed these expectations. One could expect that Si in the molten alloy would react with the free carbon and form SiC. Thus, one would get rid of the infiltration impeding carbon and concomitantly form a new phase that should enhance the hardness of the composite.

The purpose of this work was to examine the validity of these expectations. First, a thermodynamic analysis of the system confirmed the initial premise. A series of B<sub>4</sub>C preforms were prepared at ENSM-SE with different levels of porosity and free carbon content. In parallel, excess carbon-free boron carbides preforms were manufactured at the Ben-Gurion University. The two sets of preforms were infiltrated with the molten Cu–Si alloys. The experimental characterization of the composite material included a detailed microstructural examination and some mechanical property determinations.

## 2. Thermodynamic analysis

A calculated isothermal section of the Si–B–C system at 1400 K has recently been published by Seifert and Aldinger [7]. Over its high carbon content range, namely B<sub>4</sub>C<sub>1–x</sub> with 0.4 > x > 0, boron carbide is in two-phase equilibrium with SiC or in three-phase equilibrium with Si and SiC. Only at a much lower carbon content, do the silicon borides, S<sub>6</sub>B or Si<sub>3</sub>B, appear. Since copper does not form intermetallic compounds either with carbon or boron, it may be considered as a diluting agent of silicon. Thus the reaction of boron carbide with a Cu(Si) molten solution may be expressed as



According to the Gibbs phase rule, the number of degrees of freedom,  $f$ , for the quaternary Cu–Si–C–B system, at constant  $T$  and  $P$  is  $f = 4 - p$ , where  $p$  is the number of phases in equilibrium. If boron carbide with its extended range of composition, silicon carbide (a compound with constant composition) and a liquid Cu–Si–C–B solution are in equilibrium, the system just has one degree of freedom, namely, the composition of the melt determines the composition of the boron carbide phase. Thus, the interaction between stoichiometric boron carbide B<sub>4</sub>C and the liquid solution must lead to changes of the carbide phase composition. For a thermodynamic analysis of SiC being formed by carbon that originated in non-stoichiometric boron carbide, it is useful to treat the latter phase as a solid solution of B and C with variable composition [8]. Thus, the equilibrium in the Cu–Si–B–C system can be described

by the chemical reaction



where the brackets signify that Si is in the liquid solution and that carbon is in the B–C solid solution, within the composition limits corresponding to the stability range of the boron carbide phase.

The equilibrium constants for reaction (2) can be written as

$$K(2) = \frac{1}{a_{\text{Si}}a_{\text{C}}}, \quad (3)$$

where  $a_{\text{Si}}$  is the activity of Si in the melt and  $a_{\text{C}}$  is that of C in boron carbide.

First we consider the properties of the melt. The melt can be treated as a binary Cu–Si liquid solution since the solubility of C is extremely low and the boron content in the liquid solution is relatively low. Thus the effect C and B on the Si activity in the quaternary liquid solution may be neglected. The thermodynamic properties of the Cu–Si binary liquid solution were reported by Kubaschewski and Alcock [9] and the excess free energy of Si in the Cu–Si liquid solution at 1760 K, the temperature at which the experimental data is available, is shown in Fig. 1. The activity coefficient of silicon may be calculated according to equation  $\ln \gamma_{\text{Si}} = \Delta G_{\text{Si}}^E / RT$  and the activity coefficient at different temperatures was estimated using the regular solution approach

$$\text{according to which } \frac{\ln \gamma(T_1)}{\ln \gamma(T_2)} = \frac{T_2}{T_1}.$$

The carbon activity in non-stoichiometric boron carbide, according to our previously reported data [8], may be expressed by

$$\ln a_{\text{C}} = \ln X_{\text{C}} + \frac{-445\,000}{RT} [(1 - X_{\text{C}})^2 - 0.64] + 1.609, \quad (4)$$

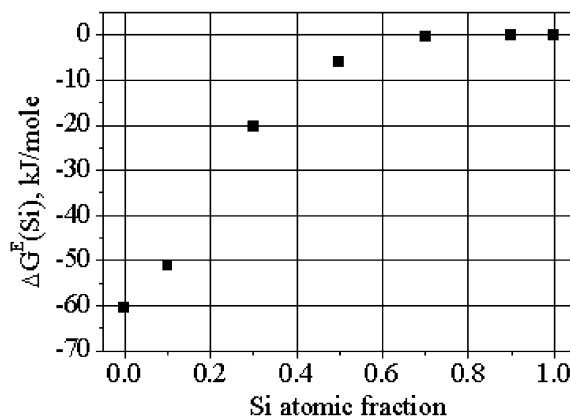


Fig. 1. The excess free energy of Si in the Cu–Si liquid solution at 1760 K.

where  $X_C$  is the carbon atomic fraction in boron carbide.

According to Ref. [10], the free energy for SiC formation from liquid Si and graphite may be expressed by equation  $\Delta G(2) = -73054 + 0.74T$ . The values of 39800 kJ/mol for the enthalpy of fusion of Si and 1687 K for its melting point, were used for calculations.

The resulting equilibrium relationships at 1523 K are presented in Fig. 2. Each point on the curve corresponds to the certain boron carbide composition in equilibrium with the liquid Cu–Si solution at a definite composition. According to Fig. 2, a liquid solution that contains more than 15 at% of Si reacts with boron carbide and as a result of this reaction, the silicon carbide phase is formed from the carbon originally present in the boron carbide phase.

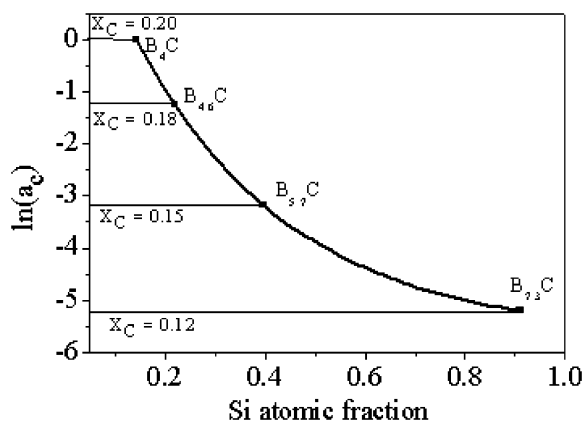


Fig. 2. Phase equilibria in the boron carbide–Cu–Si melt system at 1523 K.

### 3. Experimental

#### 3.1. Preparation of samples

The boron carbide that was used at ENSM-SE (Tetrabor 3000F, ESK Kempton) had the following specifications: B+C content 98%, O 1.3%,  $B_2O_3$  0.25%, Fe 0.03%, and Si 0.08%. The 99.9% of the particles had a grain size  $<3.1 \mu\text{m}$ , with 75%  $<1 \mu\text{m}$  and 50% had a value between 0.7 and  $0.8 \mu\text{m}$  and the specific area was  $>12 \text{m}^2/\text{g}$ . This powder was used to prepare a slurry according to the following procedures: first, the boron carbide powder was mixed with a dispersant (phosphoric ester, 1.5 wt%) and the solvent (methyl ethyl keton/ethanol 66/34). The slurry then underwent ultrasonic disagglomeration and was homogenized in a blender with SiC cylinders for 8 h. Next, a sintering agent (phenol-formaldehyde resin, Alnovol PN320) was added and the mixture was again homogenized in the blender for one night. In some instances, a pyrolysable pore-generating agent PFA (corn starch, ref.695111, Roquette, France) was also added and the mixture homogenized in the blender for 4 h at low speed. The slurry mixtures were dried under air and then under vacuum at  $100^\circ\text{C}$  and  $200 \mu\text{m}$  size particles were sifted out. Samples were prepared by uniaxial pressure at 60 MPa followed by cold isostatic compression at 350 MPa and debinded under an argon flow. Sintering was performed under an argon flow at  $2150^\circ\text{C}$  for 1 h. The initial composition and the porosity data regarding the ENSM samples that were examined are summarized in Table 1. The sample denoted T' differs from the M' samples by its lower resin content and the absence of the pore-generating agent. The residual concentration of excess carbon ranged from 3 to 4.5 wt%.

Table 1

The porosity of the ENSM-SE  $B_4C$  preforms before infiltration and of the  $B_4C$ -(Cu,Si) composite, after infiltration

Sample	Initial volume (%)	Porosity prior infiltration (%)		Porosity after infiltration (%)	Infiltration	Remarks
	Resin PFA	Open	Closed			
M1	9 7	10	3	0.0	Partial	Large free carbon inclusions
M2	9 14	13.5	1.5		Incomplete	Fine structure of the infiltrated region
M3	9 21	17	2	0.4	Complete	Fine structure
M5	9 33	17	1.3	3.1	Incomplete	Fine structure of the infiltrated region
T2	6	12.3	1.2	0.9	Partial	Large carbon inclusions

Table 2  
Chemical compositions of the boron carbide powder (wt%) used at BGU

Element or compounds	B <sub>2</sub> O <sub>3</sub>	Si	N	O	C			B	Total <sup>a</sup>
					Combined	Free	Total		
Starck	0.46	0.09	0.426	2.04	20.69	1.28	21.97	74.96	99.94
MJ	0.05	0.7	0.12	0.6	19.80	0.90	20.5	77.8	99.77

<sup>a</sup>The balance consists of Al, Fe, Ca and other unidentified impurities.

The chemical compositions of the boron carbide powder that was used at the Ben-Gurion University, (Starck), as determined by the ICP-OE method is shown in Table 2. The average particle size, the B/C ratio and the specific surface area (BET), determined by the supplier, were 0.8 μm, 3.7–3.8 and 15–20 m<sup>2</sup>/g, respectively. The powder in the absence of any binder was uniaxially compacted under 80 MPa pressure and sintered under an argon gas flow in the 2150–2200°C temperature range for 1 h, yielding porous samples with 70–95% relative density.

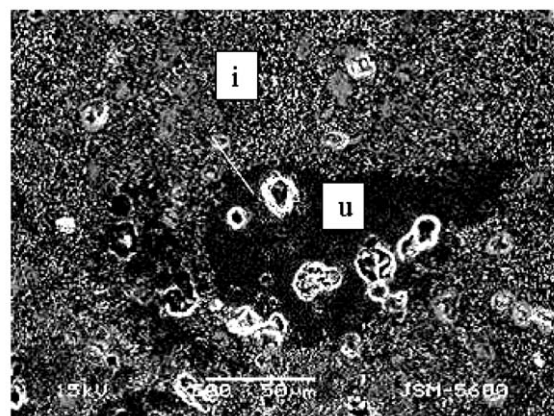
### 3.2. Infiltration and characterization

The Cu–Si metal alloy was prepared before infiltration by co-melting appropriate amounts of Si and Cu. The copper was supplied by Alfa Aesar<sup>®</sup>, 5N purity and the silicon was taken from electronic purity Si wafers. The closed porosity of the samples boron carbide preforms at ENSM-SE was determined by helium pycnometry. The apparent density was determined by the liquid displacement method in water. The open density was determined from the measured values. At BGU the open and closed porosity were determined by the liquid displacement method, as described in Ref. [11].

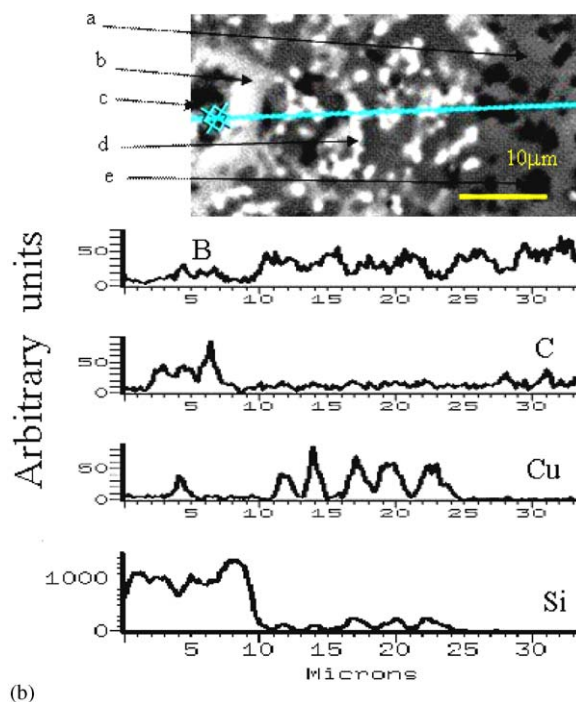
The preparation of the composites for microstructural examination was carried out according to the recommendation of Buehler LTD (Specimen Number BB11A). It consisted of several stages: (i) Planar grinding with 30 μm diamond on METLAP 10. (ii) Sample polishing by: (a) perforated Textmet with 9 μm diamond, (b) nylon with 3 μm diamond; (c) ultrapol with 1 μm diamond paste (stage #2 was carried out using METADI LUBRICANT FLUID). (iii) Polishing on Chemomet with 0.05 μm colloidal silica.

## 4. Results and discussion

The initial infiltration trials were reasonably successful, in the sense that contrary to unalloyed copper, the Cu–Si alloy penetrated the porous boron carbide preform. The results of the microstructural examination of sample M2 with roughly 15% initial porosity are shown in Figs. 3a and b. This sample underwent partial



(a)



(b)

Fig. 3. (a) Optical micrograph of a region of the cermet in which both infiltrated (i) and uninfiltrated (u) areas were present. The bright dot-like areas in the infiltrated part of the composite are cross-sections of the channels filled with the molten alloy. The large dark gray islands in the same region indicate the initial excess carbon particles that have partly or fully reacted with the Cu–Si alloy that formed a SiC-rich belt. (b) An EDS scan was performed along the thin bright straight line running from the uninfiltrated to the infiltrated area in (a). Region denoted (a) corresponds to the excess carbon in the ENSM-SE boron carbide, (b) is the Si-rich belt, (c) corresponds to the Cu–Si alloy infiltrated in the (d) porous boron carbide and (e) denotes the uninfiltrated pores that may contain some excess carbon. Of particular interest is the distribution of Si along the scanned line.

infiltration and one can clearly distinguish between the infiltrated and the non-infiltrated regions.

In sample M2, which contained excess carbon, the molten Cu–Si alloy reacted with free carbon particles in the partially sintered boron carbide and formed a surrounding SiC envelop. At the resolution that was available, it has not been possible to ascertain whether some boron, originating in the  $B_4C$ , had dissolved in the Cu channels.

X-ray diffraction revealed, as expected the presence of the  $B_4C$  matrix and of several intermetallic compounds that are present in the Cu–Si binary diagram, Fig. 4. Clearly, the metallic component is not in equilibrium state and reflects the rather rapid cooling from the molten state. During infiltration stage, the molten metal reacted with the ceramic preform yielding a fraction of SiC, in samples M2 and M3. The SiC volume fraction was much reduced in the samples M1, M5 and T1, even though none of the processing parameters had been intentionally changed in the course of the infiltration stage.

The hardness values of the infiltrated composites prepared using excess carbon containing preforms

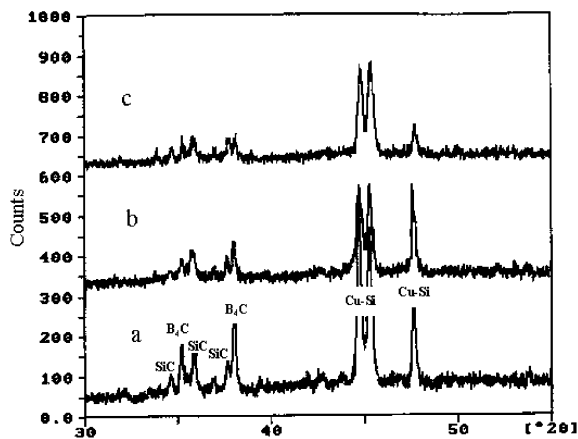


Fig. 4. XRD patterns of infiltrated  $B_4C$ -Cu(Si) composites heat-treated at  $1100^\circ C$  for (a) 2 h; (b) 4 h; and (c) 10 h.

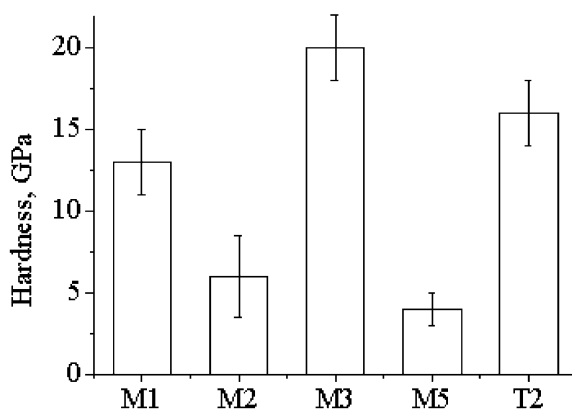
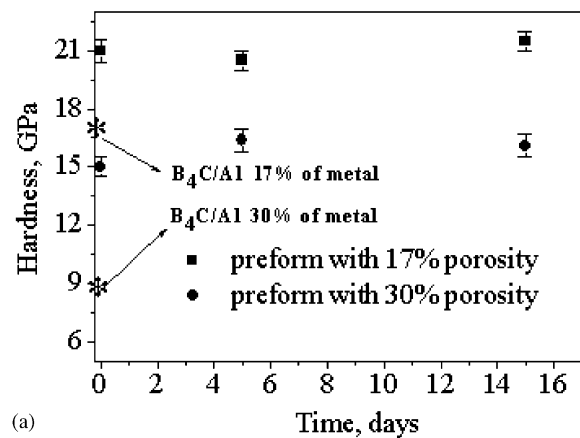


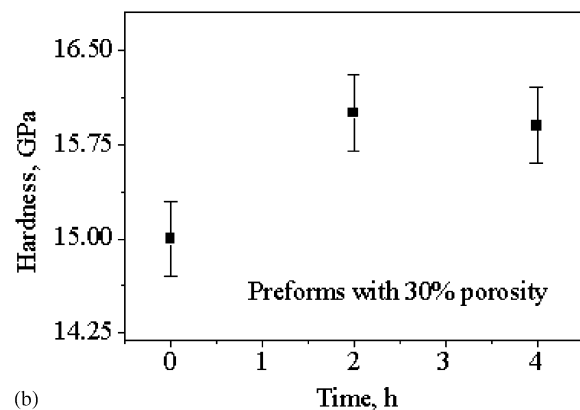
Fig. 5. Vickers hardness values of the infiltrated composites, fabricated at ENSM-SE, under 2000 g load.

fabricated at ENSM-SE displayed very large hardness fluctuations, as shown in Fig. 5. Boron carbide preforms, with no excess carbon, fabricated at BGU with 17 and 30 vol% porosity, respectively, were heat-treated at  $750^\circ C$  and  $1100^\circ C$  in evacuated quartz capsules after infiltration (Figs. 6a and b). The hardness of the composites was significantly higher than that of the previous set of composites with the same metal/ceramic ratio (Fig. 5). It is also higher than the hardness of  $B_4C$ -Al composites, as reported in the literature [12]. Heat treatment at  $1100^\circ C$  led to only a marginal increase of hardness.

In order to gain a better insight into the wetting behavior of Cu-based alloys on boron carbide substrates, we have examined cross-sections of the interface between a solidified Cu–Si alloy and a quasi-fully dense substrate, shown in Figs. 7a and b for two alloys with different Si content. The molten alloy was in contact with the substrate at  $1523^\circ C$  for 30 min, namely under conditions corresponding to the infiltration process. Examination of the microstructure suggests that increasing the Si content of the melt generates a continuous SiC layer. A thin ( $<1 \mu m$ ) Cu alloy layer



(a)



(b)

Fig. 6. The Vickers hardness values of infiltrated boron carbide preforms (manufactured at BGU) with 17% and 30% initial porosity as a function of the duration of a treatment carried out (a) at  $750^\circ C$ ; (b) at  $1100^\circ C$ .

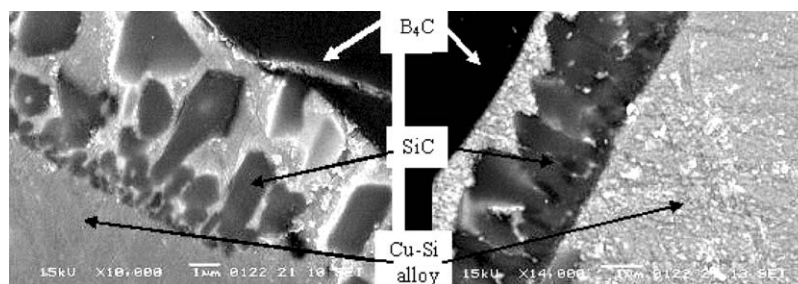


Fig. 7. The interface between the  $B_4C$  substrate and a Cu(Si) molten alloy for two different alloy compositions: (a) Cu–18.6at% Si alloy; (b) Cu–27.7at% Si alloy.

appears to be trapped between the  $B_4C$  substrate and the SiC shell. The sharp interface on the side of the SiC layer opposite to the  $B_4C$  substrate and which appears to be the location of its initial nucleation of the SiC compound is also noteworthy. This raises the possibility that SiC nucleated within the molten metal at a location at which the product of the boron and carbon activities corresponded to the equilibrium constant of Eq. (2). The presence of the thin Cu–Si layer, between the original  $B_4C$  phase and the newly formed SiC, suggests that the growth of the SiC layer proceeded via a liquid-mediated growth mechanism.

In principle, according to the thermodynamic analysis and Fig. 2, the boron carbide substrate adjacent to the Cu–Si melt should be depleted in carbon. The significant amount of SiC that was formed required a commensurate amount of carbon originating in the boron carbide matrix. Had this carbon been the result of the decomposition of the boron carbide, the excess boron—fourfold the amount of carbon present in the SiC layer—would have appeared in the solidified molten metal matrix either in the form of excess boron or in the form of boron silicides. No unalloyed boron or boron silicides were detected either by diffractometry or by EDS analysis. Auger depth profiling, however, revealed a significant increase of the boron-to-carbon ratio in the region adjacent to the carbide–molten metal interface [6]. We thus concluded that the boron carbide adjacent to the Cu–Si alloy is carbon-depleted, in agreement with the conclusions of the thermodynamic analysis, as shown in Fig. 2.

The SiC layer consists of mostly columnar SiC grains surrounded by some residual, Si-depleted Cu. Presumably this is also the structure of the belt-like rings that surround the large carbon-rich inclusions in those regions of the composite matrix in which infiltration by the molten alloy did take place. This layer, consisting essentially of SiC, acts as a diffusion barrier and impedes the diffusion of elements from or to the reaction front and further formation of SiC within the metal matrix. This feature may be the reason for the limited effect of the heat treatment on the composite hardness.

## 5. Conclusions

The use of Cu–Si alloys significantly improves the wetting of boron carbide preforms as compared to wetting by unalloyed copper. Boron carbide porous preforms were successfully infiltrated by the Cu–Si alloy, even though the infiltration in some instances was incomplete. The molten alloy reacts with the excess carbon present in the boron carbide to form SiC that acts as a barrier around the carbon particles and impedes the completion of this reaction. SiC is also formed in boron carbide preforms with no excess carbon, suggesting that Si reacts with carbon of the  $B_4C$  matrix. The formation of the surface barrier around the boron carbide particles and the low rate of the reaction between  $B_4C$  and the molten alloy account for the limited increase of hardness as a function of the duration of the heat treatments. One would also conclude that the ENSM-SE approach for fabricating boron carbide preforms to be used for infiltration with a Cu(Si) alloy is not useful, since the excess carbon impedes good infiltration by lowering the wetting by this alloy.

## Acknowledgments

We wish to thank Mr. G. Saharov for his able assistance. This work was partly supported by Israeli Ministry of Science Grant No. 20562-01-99.

## References

- [1] A.J. Pyzik, I.A. Aksay, M. Sarikaya, in: J.A. Pask, A.G. Evans (Eds.), *Materials Science Research*, Vol. 21, Microstructures '86, Plenum Press, New York, 1987, p. 45.
- [2] D.C. Halverson, A.J. Pyzik, I.A. Aksay, W.E. Snowden, *J. Am. Ceram. Soc.* 72 (1989) 775–780.
- [3] D.C. Halverson, A.J. Pyzik, I.A. Aksay, Boron carbide aluminum and boron carbide-reactive metal cermets, US Patent no. 4,605,440, 1986.
- [4] A.J. Pyzik, R.T. Nilsson, Boron-carbide-copper cermets and method for making same, US Patent no. 5,145,504, 1991.

- [5] T. Maruyama, S. Onose, *J. Nucl. Sci. Technol.* 36 (1999) 380–385.
- [6] N. Froumin, N. Frage, M. Aizenshtein, M.P. Dariel, *J. Euro. Ceram. Soc.* 23 (2003) 2821–2828.
- [7] H.J. Seifert, F. Aldinger, in: M. Jansen (Ed.), *Structure and Bonding—High Performance Non-Oxide Ceramics*, Vol. 101, Springer, Berlin, 2002, p. 1.
- [8] L. Levin, N. Frage, M.P. Dariel, *Metal. Mater. Trans. A* 30A (1999) 3201–3210.
- [9] O. Kubaschewski, C.B. Alcock, *Metallurgical Thermochemistry*, 5th Edition, Pergamon Press, Oxford, 1979.
- [10] JANAF Thermochemical Tables, *Handbook of Chemistry and Physics*, National Bureau of Standards, Gaithersburg, MD, 1985.
- [11] D.R. Askleland, *The Science and Engineering of Materials*, 3rd Edition, Chapman & Hall, London, 1996.
- [12] A.J. Pyzik, D.R. Beaman, *J. Am. Ceram. Soc.* 78 (1995) 305–312.